Journal of
ALLOYS
AND COMPOUNDS

An Interdisciplinary Journal
of Materials Science and
Solid-State Chemistry and Physics

An optimum path to obtain β Cu–Zn–Al by mechanical alloying

F.G. Sesma [a,b], F.C. Gennari [a,b,c], J. Andrade-Gamboa [c], J.L. Pelegrina [a,b,d],*

[a] Centro Atómico Bariloche, Av. E. Bustillo 9500, R8402AGP San Carlos de Bariloche, Argentina
[b] Consejo Nacional de Investigaciones Científicas y Técnicas, Argentina
[c] Departamento Fisicoquímica de Materiales, Centro Atómico Bariloche, CNEA, Av. E. Bustillo 9500, R8402AGP San Carlos de Bariloche, Argentina
[d] División Física de Metales, Centro Atómico Bariloche, CNEA, Av. E. Bustillo 9500, R8402AGP San Carlos de Bariloche, Argentina

ARTICLE INFO

ABSTRACT

Cu–Zn–Al alloys have been produced by low energy ball milling following six different synthesis paths. In all cases, a mixture of α and β phases have been obtained. Milling for 100 h without interruptions the three elements simultaneously gave the best ratio between the amount of β phase and the milling time. Low temperature thermal treatments to the powders (up to 450 °C) lead to γ phase crystallite growth, with the amount of β phase remaining nearly constant. With anneals at 800 °C the β phase fraction in the powder increased solely to 86%. A sample of pure β phase was obtained only after warm compaction at 680 MPa and sintering at temperatures above 800 °C. In addition, it was necessary to reach temperatures of 900 °C in order to have a material that transforms martensitically.

© 2013 Elsevier B.V. All rights reserved.

1. Introduction

Mechanical alloying is one of the most popular non-equilibrium processing techniques of solids due in part to the high homogeneity achieved in the resulting products [1]. Therefore, the preparation of shape memory materials by mechanical alloying has attracted a high interest because transformation temperatures are strongly composition dependent. This has been successfully achieved for binary Ni–49.7 at%Ti [2] as well as for ternary Cu–27.6 at%Al–3.6 at%Ni [3]. In both cases the pure elements in the form of powders were used as the starting material and were mechanically milled for different times under an Ar atmosphere. The milled powders were then compacted, sintered, further annealed at high temperature and water quenched. The samples obtained in this way presented the martensitic transformation and characteristic temperatures were determined using differential scanning calorimetry [2,3].

A similar alloying and consolidation procedure has been employed to obtain the quaternary Cu–24.2 at%Al–4.6 at%Ni–2.0 at%Mn alloy [4]. In this case the minority element was added with the intention of enhancing the thermoelastic and pseudoelastic properties, as reported in [5]. With this alloy a 100% shape memory recovery efficiency was obtained [4], which did not degrade after 100 cycles.

An alternative way for the preparation of shape memory alloys starts from pre-alloyed powders of different compositions instead from the pure elements. Commercial Cu–30 at%Zn, Cu–14 at%Zn and elemental Al powders have been milled to obtain Cu–25.5 at%Zn–5.5 at%Al and Cu–21.1 at%Zn–11.2 at%Al alloys [6]. Four stages were identified during the milling process which led to the formation of an homogeneous powder, but no martensitic transition was reported. In a similar way, a Cu–27.1 at%Al–3.0 at%Ni was produced from two pre-alloyed ternary Cu–Al–Ni alloys of different compositions [7]. The compacts were obtained by hot isostatic pressing. In this latter alloy, several thermomechanical treatments were necessary to obtain the martensitic transition responsible of the shape memory effect.

The martensitic transformation in Cu–Zn–Al alloys occurs between the austenite and the martensite. The former has a body centered cubic structure at high temperatures (the β phase) while the latter is usually described as a stacking of close packed planes. The β phase can be retained metastably at room temperature because it builds up long range order in first and second neighbors. In this latter case the phase is called β_3 (L2$_1$ order). It competes in stability with the α and γ phases, as can be seen from the phase diagram at 700 °C shown in Fig. 1 [8]. The Cu-rich α phase is face centered cubic while γ is complex cubic [9]. It is important to mention that in the above commented work [6], only α and γ phases were obtained. To our knowledge, no work in the literature refers to the synthesis of β_3 Cu–Zn–Al alloys. The interest in this subject

* Corresponding author at: Centro Atómico Bariloche, Av. E. Bustillo 9500, R8402AGP San Carlos de Bariloche, Argentina. Tel.: +54 294 4445272; fax: +54 294 4445299.
E-mail address: jlp201@cab.cnea.gov.ar (J.L. Pelegrina).

Fig. 1. Isothermal section at 700 °C of the Cu–Zn–Al phase diagram.

The chemical composition of the resulting powders was analyzed in a Philips SEM 515 using an EDAX energy dispersive spectrometer.

Six different synthesis sequences to obtain a nominal composition of Cu–18.4 at%Zn–13.7 at%Al were tested. They are:

A. The three elements were milled simultaneously from the beginning. The sampling was done after certain periods of processing and investigated by XRPD (Fig. 2a). The milling step was finished (after 80 h) when the position of the α phase diffraction peaks was found to reach asymptotic values as shown in Fig. 2b. It has been verified that the XRPD peak width also reaches an asymptotic value at the same milling times.

B. A blend of Cu and Zn was milled to obtain a Cu–21.32 at%Zn alloy, following the relative composition that these elements have in the ternary alloy. After determining the completion of this alloying step with a similar criterion as mentioned in relation to Fig. 2b, the proper amounts of the Cu–Zn binary powder and Al flakes were milled next until the ternary alloy was obtained.

C. In a similar way as in the previous point, a blend of Cu and Al was milled to obtain a Cu–16.79 at%Al. Next, the proper amounts of the Cu–Al binary powder and Zn filings were milled.

D. An equiatomic blend of Cu and Zn was milled to obtain a β_2 (B2 order) phase alloy. In the following milling step it was necessary to add Cu and Al to reach the composition of the ternary alloy.

E. As in the previous point, a Cu–50 at%Zn alloy was formed first. Next, Cu was added in an amount which avoids a reduction of e/a below 1.46. After mechanical milling the mix for 10 h, a small amount of Al was included and milled again for 10 h. In this case the limiting value of e/a was 1.53. This process was repeated adding Cu and Al by turns, until the total added components complete the nominal composition of the ternary alloy. This was achieved after 11 steps, which involved a total of 110 h of milling. No sampling was performed in the intermediate steps. This complex sequence was selected in order to maintain the resulting powder within the limits of the β phase field shown in Fig. 1.

F. The three elements were milled simultaneously as in sequence A, but without intermediate sampling and during 100 h. A higher time than in A was used, because previous milling experience in other materials indicated that

comes from the possibility of formation of a phase at room temperature, whose stability is not well established below 300 °C [8]. Normally, the β_3 phase is obtained from the melt and, at an e/a of 1.48, is retained metastably at room temperature without the need of rapid cooling. As the β phase is prone to rapid grain growth, it is difficult with this production method to obtain grain sizes below 3 mm diameter, which degrades the mechanical properties, unless grain refiners are used. In the cases where small amounts of Co, Ti or B have been added, the grain sizes were reduced to around 100 μm [10,11]. In another work, grain sizes down to 25 μm were obtained by adding Zr [12]. Without the inclusion of refiners, grain sizes of 13 μm were found in melt-spun ribbons [13]. Therefore, an additional interesting point in the preparation of a Cu–Zn–Al β_3 phase alloy by mechanical alloying is to explore the possibility of obtaining nano-sized crystallites.

In the present work several sequences of milling elemental Cu, Zn and Al powders were applied in order to explore different synthesis paths to produce a β phase alloy. In these experimental series, it were also considered sequences that synthesize first binary alloys. Therefore, from the information retrieved through these different synthesis procedures it was tested the possibility of having an optimum milling path that enhance the amount of the austenitic phase in the final powder.

2. Experimental

Filings of pure (99.99%) Cu and Zn, and Al flakes were used as the starting materials. The mechanical alloying was carried out in an Uni-Ball-Mill II equipment manufactured by Australian Scientific Instruments (Canberra, Australia). It has a rotating cylindrical cell of around 200 mm diameter and 29 mm height made of hardened steel. Seven bearing balls of 25.4 mm diameter were used with 10 g of material, resulting in a powder-to-ball ratio of nearly 47. An Ar atmosphere with an overpressure of around 0.5 MPa and a rotation speed of 177 rpm were used. At each sampling, 200 mg of powder was removed. The powder was scrapped from the walls when agglomeration and sticking effects were observed. Afterwards, the Ar atmosphere was established again.

Structural and microstructural characterization were performed by X-ray powder diffraction (XRPD) with a Philips PW1710/01 diffractometer using Cu Kα radiation and a graphite monocromator. The scans were recorded between 25° and 100° using a step of 0.02° and a counting time of 1 s, allowing the determination of the lattice parameter with an uncertainty of 2×10^{-5} nm. Si was used as an external pattern for the 2θ calibration. A preliminary Hall–Williamson analysis has shown that microstrains were negligible in the powders. Therefore, crystallite sizes of α, β and γ phases were calculated through the Scherrer equation, fitting a Lorentzian function to the reflections (1 1 1), (1 1 0) and (3 2 1), respectively. The relative amount of phases was determined from the same peaks of each phase using the direct comparison method [14].

Fig. 2. (a) X-ray diffractograms after milling the three elements simultaneously for different times. The patterns were shifted vertically for clarity. (b) Angular position of the selected diffraction peaks of the α phase, normalized by their value at 80 h, as a function of milling time.

alloying was more efficient when it was periodically interrupted for sampling [15]. No further changes were found after milling during additional 40 h.

Thermal treatments of the milled powders below 500 °C were carried out using a TA 2910 differential scanning calorimeter (DSC). Temperature scanning rates of 5 K/min and an Ar flow of 120 ml/min were used. Around 60 mg of powder was placed in an Al pan, while an empty pan was used as the reference.

Thermal treatments of the milled powders at 800 °C were made in a sealed fused silica tube under argon atmosphere in a resistance furnace.

Some of the powders were consolidated in a 6 mm diameter die to form disc-shaped compacts. A first set of experiments (with powder from sequence A) was done at 50 °C applying pressures of up to 1400 MPa during 10 min using an hydraulic press. The green compacts were then sintered at 800 °C for 30 min. A second procedure (with powder from sequence F) consisted of applying a pressure of 680 MPa at 100 °C, increasing then to 200 °C maintaining the load and ageing for different periods. This process is known as warm compaction [16]. To this end an Instron 5567 testing machine with an Instron 3119-005 temperature chamber was used. In all cases the walls of the die and the punches were lubricated with grease to allow an easier ejection of the compact.

The density of the compacts was determined using the mass and a geometrical estimate of its volume.

3. Results and discussion

In the following, the name of β phase will be used independent of the degree of long range order presented by the particular alloy, which agreed with the expected from the particular composition.

3.1. Precursor two-component alloys (binary steps)

Except for the sequences A and F, in the four remaining cases (B–E) there is an initial step in which two elements are milled to form a binary alloy. After the asymptotic value of the diffraction peak position was reached, a comparison of the measured cell parameter and the calculated for the corresponding nominal composition was made. To this end a linear fit of the experimental data for α and β Cu–Zn [17] was proposed

$$a_\alpha(\mathrm{nm}) = 0.3614 + 0.000228 \text{ at\%Zn} \tag{1}$$

$$a_\beta(\mathrm{nm}) = 0.2848 + 0.000224 \text{ at\%Zn} \tag{2}$$

as also for α Cu–Al [18]

$$a_\alpha(\mathrm{nm}) = 0.3614 + 0.000259 \text{ at\%Zn} \tag{3}$$

The time to complete the sequence and the cell parameters (measured and expected) are presented in Table 1. It can be seen that in about 40 h the binary phases in the Cu–Zn system are formed, whereas in Cu–Al a factor of six larger time is needed. The excellent agreement between the experimental and expected values for the final two-component materials is an indication of the high quality of the alloying process. The crystallite sizes, also shown in Table 1, fall in the range from 10 to 20 nm. This warranted similar initial conditions in the following milling step for the synthesis of the ternary alloy.

3.2. Three-component products of each alloying sequence (ternary steps)

In the six cases the milled powders were a mixture of α and β phases, with no traces of γ or any other phase, crystalline or amorphous. In Table 2 are presented the partial times needed for completion of the milling sequences, together with the total time resulting from the sum of both consecutive steps (binary and ternary). It can be seen that the less time consuming process is that of milling simultaneously the three pure elements. On the other hand, the maximum amount of β phase is obtained through milling sequence E, with a 34%, after 150 h of milling (Table 2). However, if the ratio between the phase fraction and the total milling time is used as the definition of alloying efficiency, sequence F results the optimum path.

In Table 2 they are also reported the crystallite sizes and lattice parameters of α and β phases. The α phase crystallites show sizes and lattice parameters that are independent of the milling sequence, with mean values of 10 nm and 0.3695 nm, respectively. On the other hand, the β phase crystallite sizes present a bigger scatter, between 4 nm and 13 nm, and the lattice parameters span a greater range of values, being bigger for the two smaller crystallite sizes. No reason for this latter observation was found. If Eqs. (1) and (3) are merged into one, following the conclusions in [19] and taking only first order composition terms, an α lattice parameter of 0.3691 nm can be calculated for the nominal composition. This value is in good agreement with those reported in Table 2. For the lattice parameter of β, the formula deduced from the volume per atom and reported in [20] was used, resulting in 0.2918 nm for the nominal composition, also in reasonable agreement with the present results. It is interesting to remark that a better agreement is obtained for the synthesis sequences A and F. This could have been taken as an indication that the nominal alloy composition can be more easily reached when the three elements are milled simultaneously. In particular, this would have been the case for sequence F, with the additional advantage that the final composition would not be altered by the absence of intermediate sampling. Notwithstanding, an analysis of the composition of the powder resulting from sequence F by energy dispersive spectrometry revealed a higher scatter than expected. It was also found from EDS measurements that the samples were contaminated with traces of Fe and Cr from the steel in the milling cell and balls. The amount of the latter elements was around the experimental uncertainty (1 at%).

3.3. Thermal treatments

The following experiments were made using powder resulting from the optimum milling path (sequence F). In Fig. 3 two consecutive calorimetric curves between room temperature and 450 °C can be observed. As the powder is heated for the first time, there is an exothermic event between 100 °C and 400 °C, which in a second heating cycle is absent. This has been taken as evidence of the limited heating of the powder during milling, below 100 °C. On cooling no special thermal events can be observed. The change in behavior below 170 °C is an instrumental effect due to the impossibility to maintain a constant cooling rate.

With the aim to increase the β phase fraction, thermal treatments in the DSC were done. The powder was isothermally annealed at several temperatures for a period of 3 h and new X-ray diffractograms (not shown) were registered in order to analyze its evolution. The corresponding results are shown in Fig. 4. Above 100 °C the γ phase grows, the amount of β remains nearly constant and α diminishes (Fig. 4a). Note that this behavior does not necessarily mean that γ grows in detriment of α, because it is likely that the three phases mutually interact while reducing their free ener-

Table 1
Time needed to complete the milling sequences for the binary alloys, resulting crystallite sizes and lattice parameters.

Sequence	Binary step	Milling time (h)	Crystallite size (nm)	Measured lattice parameter (nm)	Expected lattice parameter (nm)
B	Cu + Zn → α	40	16	0.3664	0.3663 (Eq. (1))
C	Cu + Al → α	240	12	0.3659	0.3657 (Eq. (3))
D	Cu + Zn → β	40	18	0.2956	0.2960 (Eq. (2))
E	Cu + Zn → β	40	18	0.2956	0.2960 (Eq. (2))

Table 2
Time needed to complete the milling sequences, final amount of β phase and crystallite sizes.

Sequence	Final step	Time for the final step (h)	Total milling time (h)	Amount of β lattice (%)	Crystallite size of α phase (nm)	Crystallite size of β phase (nm)	α Lattice parameter (nm)	β Lattice parameter (nm)
A	Cu + Zn + Al	80	80	19	10	12	0.3698	0.2916
B	α (Cu–Zn) + Al	160	200	24	9	8	0.3700	0.2907
C	α (Cu–Al) + Zn	80	320	32	9	4	0.3689	0.2945
D	β (Cu–Zn) + Cu + Al	80	120	21	10	10	0.3697	0.2914
E	β (Cu–Zn) + (Cu/Al) by turns	110	150	34	11	5	0.3687	0.2967
F	Cu + Zn + Al	100	100	30	10	13	0.3700	0.2916
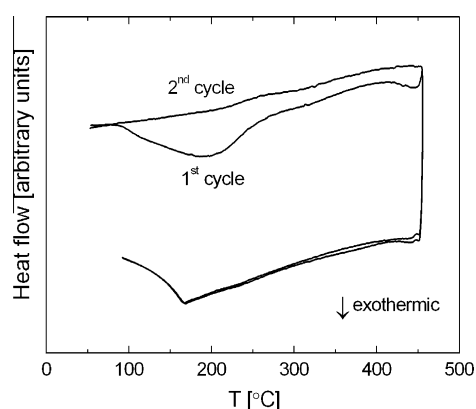
Fig. 3. Consecutive differential scanning calorimetry curves showing the exothermic evolution during the first warm up.

gies. As expected, the crystallite sizes (L) of the three phases grow with the annealing temperature as shown in Fig. 4b. By assuming a parabolic kinetics for the grain growth [21]

$$L^2 - L_0^2 = kt \tag{4}$$

where L_0 is the initial crystallite size and t is the annealing time, it was possible to estimate the activation energy Q for growth of the different phases. For the temperature-dependent rate parameter k, an Arrhenius-type equation was proposed [21]

$$k = k_0 \exp(-Q/R/T) \tag{5}$$

with k_0 a constant, T the absolute temperature and R the universal gas constant. The logarithm of k as a function of the inverse of the temperature of annealing can be seen in the inset of Fig. 4b, together with the linear fit for each phase. The resulting activation energies for grain growth are (56 ± 7) kJ/mol for α, (23 ± 4) kJ/mol for β and (41 ± 8) kJ/mol for γ; i.e. similar values for α and γ, and about 50% smaller for β.

Activation energies for grain growth have been measured in Cu-based alloys with crystallite sizes above 1 μm. In α-brass no growth was found at temperatures below or equal to 673 K [22]. For higher temperatures and using Eqs. (4) and (5) the authors obtained a value of 150 kJ/mol. In β-copper based shape memory alloys, experiments were performed at temperatures above 970 K [23,24]. In Cu–Zn–Al the activation energy was between 110 kJ/mol [23] and 150 kJ/mol [24], which was reduced to around 36 kJ/mol when Mn or Co was added to form quaternary alloys. According to the authors [23], the presence of these fourth elements would change the mechanism of diffusion to one involving cooperative atomic shuffles. Then, in the present case of agglomerates of nano-sized crystallites, significant lower growth activation energies have been measured.
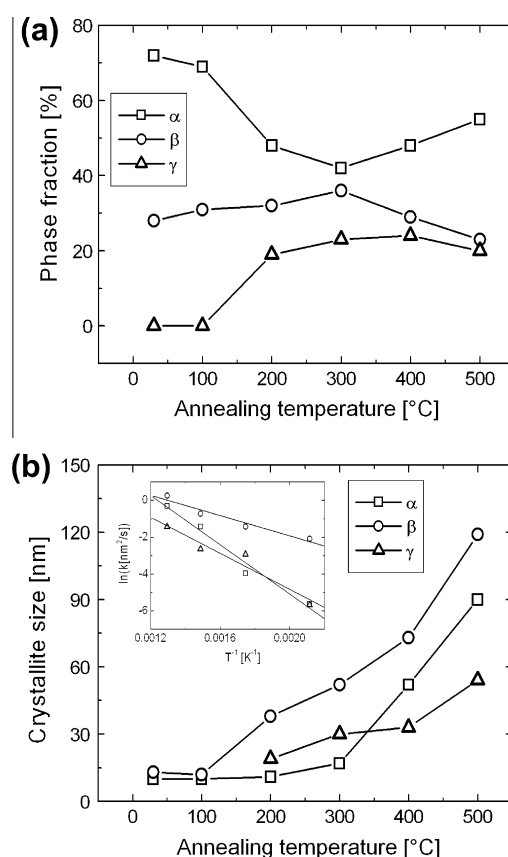

Fig. 4. Phase fraction (a) and corresponding crystallite sizes (b) as a function of the temperature at which the powders were annealed during 3 h. In (b) the inset was used for the calculation of the activation energy of growth.

The decrease of activation energy with the lowering in grain size is usually ascribed to the large amount of grain boundary enthalpy that supplies a higher driving force for the process [25,26]. It has been found in nanocrystalline Cu that this arises from a higher density of interfaces rather than to a higher grain boundary energy [26]. It was additionally invoked an enhanced grain boundary mobility due to the fact that these boundaries are non-equilibrium structures [27]. On the other hand, the grain growth is reduced or even hindered in the presence of residual porosity [27]. In the present case the high growth rate can be attributed to the existence of crystallites with nanometer dimensions and would indicate a reduced porosity in the powders.

As the amount of β does not change with the thermal treatments (see Fig. 4a), these "low temperature" annealings are not useful to enhance the β phase fraction. When the powder was annealed during 15 min at 800 °C, the γ phase disappeared and the fraction of β increased up to 86% (XRPD not shown). Heating

at the same temperature but during 24 h resulted in 89% of β, the highest limit for practical purposes.

It is to be noted that the increase of the β phase fraction could only happen within an agglomerate of crystallites of the different phases. It cannot be expected that an efficient interchange or diffusion of the elements can occur between the agglomerates in the powder. Therefore, the high amount of β obtained after the thermal treatments at high temperatures speaks about a high homogeneity in composition of the agglomerates (not composition of the crystallites).

3.4. Compaction and sintering

The apparent density of the as-milled powder was 3.3 g/cm^3. Results of supplementary compaction and sintering are shown in Fig. 5. When compacted at 50 °C at different stresses, there is a range where no density changes occur as can be seen in Fig. 5a. Subsequently, in a short stress interval the density increases to a maximum value. Notwithstanding this maximum density has a high spread, perhaps due to the low compaction temperature. The greens were afterwards sintered at 800 °C during 30 min. No further changes in density were found. Then for practical purposes the lower limit of around 700 MPa should be used for the compaction of these Cu–Zn–Al powders.

If a compaction stress of 680 MPa (a load of 2 tons) is applied at 200 °C during different hold times, a higher density increase is found, as shown in Fig. 5b. It can also be noted that the spread of the values is reduced, compared with Fig. 5a. The highest density reached of 6.9 g/cm^3 corresponds to about 88% that of the bulk alloy, which was calculated using the lattice parameter. The resulting greens present no traces of the γ phase. The amount of β phase, as also the α and β phase crystallite sizes are similar to those observed in the loose powder after the thermal treatment at 200 °C (Fig. 4b).

Additional sintering at 800 °C for 90 min did not produce any further changes in density nor swelling or shrinkage. These sintered compacts were quenched and in this case samples with only β phase were obtained. The crystallite sizes were around 600 nm. No traces of the martensitic transformation were found in these samples, within the detection capability of DSC experiments.

In a previous work, a Cu–Al–Ni powder alloy has been compacted at 900 MPa and then sintered in a stress free state at 950 °C for 20 h [3]. A maximum density of 6.4 g/cm^3 was obtained, which corresponds to a relative density of 90%. In [3] mean grain diameters between 500 nm and 2000 nm were reported for the sintered compacts. Also green compacts of up to about 96% relative density has been obtained in Cu–Al–Ni–Mn [4,28]. In this case, the powders were simultaneously compacted at a pressure of 30 MPa to 40 MPa and heated at temperatures between 850 °C and 950 °C. A mean grain diameter of 3000 nm was reported for the compact sintered at 850 °C [4]. In both, ternary and quaternary alloys, the martensitic transformation was detected and the shape-memory effect could be measured.

In the present work the stress was applied at low temperatures, minimizing microstructural coarsening, with the aim to improve the characteristics of the green through the higher growth rate of the nanocrystalline sized powder. Then, the temperature of 200 °C was applied, at which it is known that the powder begins to evolve (Fig. 4). After the thermal treatment at 800 °C a pure β phase sample with crystallite sizes about 600 nm was obtained. A martensitic transformation start temperature of 263 K was expected for the nominal composition of the alloy but it was not experimentally observed. Therefore, an additional anneal at 900 °C for 25 min was performed, followed by a quench in water at ambient temperature. In spite that no further modification of the crystallite sizes nor an increase in compositional homogeneity
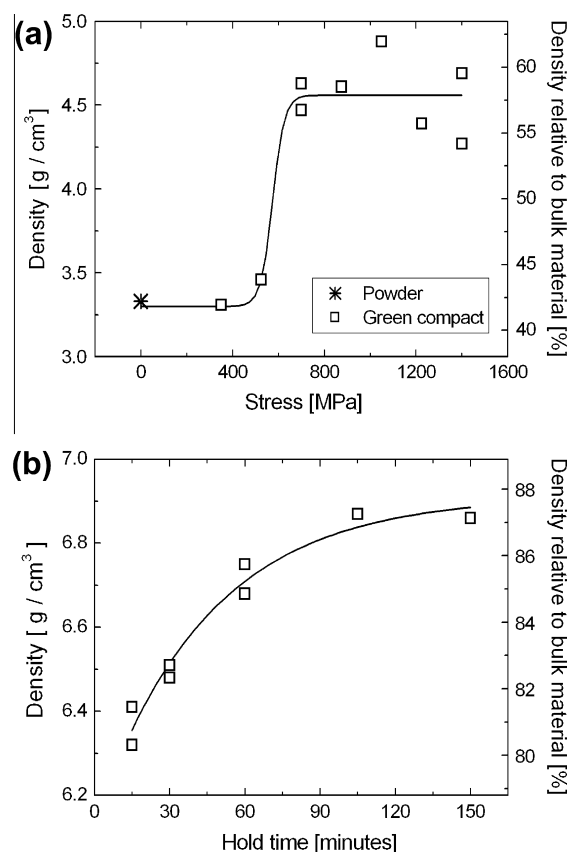

Fig. 5. (a) Density of the green compact as a function of the applied stress at 50 °C. (b) Density of the green compact as a function of the hold time of a stress of 680 MPa at 200 °C. In both figures the lines are a guide for the eyes.

could be detected, the martensitic transition appeared at a temperature of around 260 K. Notwithstanding, two characteristics indicated an anomalous behavior: the transformation range increased to about 60 K, both on cooling and on heating, and an hysteresis of about 100 K was detected. This means a factor of three and ten higher than in the conventional alloy, respectively [29]. The increased transformation range can be ascribed to the unexpected spread in composition, while the big hysteresis is more likely to be due to the small crystallite sizes.

4. Conclusions

1. The β phase of a Cu–Zn–Al alloy can be obtained from low energy ball milling following different synthesis routes.
2. In all cases the final powder also contains the α phase. The β phase mass fraction ranged from 19% to 34%.
3. The best efficiency, defined as the ratio between the obtained amount of β phase and the milling time, has been achieved when the three pure elements were milled simultaneously and continuously for 100 h.
4. The final powder presented a spread in composition that is in contradiction with the traditionally assumed homogeneity of the milling product.
5. The temperature of the powder during low energy milling does not surpass 100 °C.
6. Thermal treatments up to 450 °C did not change the proportion of β phase, while at 800 °C the amount of β phase in the powder raised up to 89%.
7. The optimum stress for compaction, at which the density did not further increase, was at around 700 MPa.

8. A 100% β phase specimen can be obtained after warm compaction at 200 °C and sintering at 800 °C, with a density close to 88% of the theoretical value and crystallite sizes in the order of 600 nm.

9. The martensitic transformation appears only after sintering at 900 °C but showing an anomalous transformation range and hysteresis, possibly due to microstructural effects.

Acknowledgements

References

[1] C. Suryanarayana, Mechanical Alloying and Milling, Marcel Dekker, New York, 2004, p. 11.

[2] W. Maziarz, J. Dutkiewicz, J. Van Humbeeck, T. Czeppe, Mechanically alloyed and hot pressed Ni–49.7Ti alloy showing martensitic transformation, Mater. Sci. Eng. A 375–377 (2004) 844–848.

[3] S.M. Tang, C.Y. Chung, W.G. Liu, Preparation of Cu–Al–Ni-based shape memory alloys by mechanical alloying and powder metallurgy method, J. Mater. Process. Technol. 63 (1997) 307–312.

[4] Z. Li, Z.Y. Pan, N. Tang, Y.B. Jiang, N. Liu, M. Fang, F. Zheng, Cu–Al–Ni–Mn shape memory alloy processed by mechanical alloying and powder metallurgy, Mater. Sci. Eng. A 417 (2006) 225–229.

[5] M.A. Morris, T. Lipe, Microstructural influence of Mn additions on thermoelastic and pseudoelastic properties of Cu–Al–Ni alloys, Acta Metall. 42 (1994) 1583–1594.

[6] S. Zhang, L. Lu, M.O. Lai, Cu-based shape memory powder preparation using the mechanical alloying technique, Mater. Sci. Eng. A 171 (1993) 257–262.

[7] A. Ibarra, J. San Juan, E.H. Bocanegra, M.L. Nó, Thermo-mechanical characterization of Cu–Al–Ni shape memory alloys elaborated by powder metallurgy, Mater. Sci. Eng. A 438–440 (2006) 782–786.

[8] G. Petzow, G. Effenberg (Eds.), Ternary Alloys: A Comprehensive Compendium of Evaluated Constitutional Data and Phase Diagrams, vol. 5, Weinheim, New York, 1992, p. 103.

[9] P.R. Subramanian, D.J. Chakrabarti, D.E. Laughlin (Eds.), Phase Diagrams of Binary Copper Alloys, American Society for Metals, Materials Park, Ohio, 1994, p. 489.

[10] R. Elst, J. Van Humbeeck, M. Meeus, L. Delaey, Grain-refinement during solidification of β-Cu based alloys, Z. Metallkde. 77 (1986) 421–424.

[11] H. Morawiec, Z. Bojarski, J. Lelatko, K. Joszt, Grain refinement of Cu–Zn–Al shape memory alloys, Z. Metallkde. 81 (1990) 419–423.

[12] J.S. Lee, C.M. Wayman, Grain refinement of Cu–Zn–Al shape memory alloys, Metallogr 19 (1986) 401–419.

[13] J.L. Pelegrina, L.M. Fabietti, A.M. Condó, G. Pozo López, S.E. Urreta, The influence of microstructure on the martensitic transformation in Cu–Zn–Al melt-spun ribbons, Philos. Mag. 90 (2010) 2793–2805.

[14] Y. Waseda, E. Matsubara, K. Shinoda, X-Ray Diffraction Crystallography, Springer, Berlin, 2011, p. 153.

[15] F.C. Gennari, unpublished results.

[16] R.M. German, Powder Metallurgy and Particulate Materials Processing, Metal Powder Industries Federation, Princeton, 2005, pp. 209–210.

[17] P.R. Subramanian, D.J. Chakrabarti, D.E. Laughlin (Eds.), Phase Diagrams of Binary Copper Alloys, American Society for Metals, Materials Park, Ohio, 1994, p. 493.

[18] P.R. Subramanian, D.J. Chakrabarti, D.E. Laughlin (Eds.), Phase Diagrams of Binary Copper Alloys, American Society for Metals, Materials Park, Ohio, 1994, p. 31.

[19] T.B. Massalski, H.W. King, Alloy phases of the noble metals, Prog. Mater. Sci. 10 (1963) 3–78.

[20] R. Romero, J.L. Pelegrina, Change of entropy in the martensitic transformation and its dependence in Cu-based shape memory alloys, Mater. Sci. Eng. A 354 (2003) 243–250.

[21] C. Suryanarayana, C.C. Koch, in: C. Suryanarayana (Ed.), Non-equilibrium Processing of Materials, Pergamon, 1999, pp. 323–324.

[22] S.P. Toppo, C.C. Jyotsna, B.P. Kashyap, Flow behaviour and microstructural evolution in cold worked 70:30 α-brass, Mater. Sci. Technol. 27 (2011) 136–144.

[23] F.J. Gil, J.M. Guilemany, J. Fernández, Kinetic grain growth in -copper shape memory alloys, Mater. Sci. Eng. A 241 (1998) 114–121.

[24] F.J. Gil, J.M. Guilemany, Effect of cobalt addition on grain growth kinetics in Cu–Zn–Al shape memory alloys, Intermet 6 (1998) 445–450.

[25] B. Günther, A. Kumpmann, H.-D. Kunze, Secondary recrystallisation effects in nanostructured elemental metals, Scripta Metall. Mater. 27 (1992) 833–838.

[26] Y.K. Huang, A.A. Menovsky, F.R. de Boer, Calorimetric analysis of the grain growth in nanocrystalline copper samples, Nanostruct. Mater. 2 (1993) 587–595.

[27] V.Y. Gertsman, R. Birringer, On the room-temperature grain growth in nanocrystalline copper, Scripta Metall. Mater. 30 (1994) 577–581.

[28] Z. Xiao, Z. Li, M. Fang, S. Xiong, X. Sheng, M. Zhou, Effect of processing of mechanical alloying and powder metallurgy on microstructure and properties of Cu–Al–Ni–Mn alloy, Mater. Sci. Eng. A 488 (2008) 266–272.

[29] J.L. Pelegrina, R. Romero, Calorimetry in Cu–Zn–Al alloys under different structural and microstructural conditions, Mater. Sci. Eng. A 282 (2000) 16–22.